Anal. Chem. **2007,** *79,* 1266−1270

Correspondence

Nanobiosensor Design Utilizing a Periplasmic *E. coli* Receptor Protein Immobilized within Au/Polycarbonate Nanopores

Abhinav Tripathi,[†] Jianbin Wang,[†] Linda A. Luck,[‡,§] and Ian I. Suni*[,†]

Department of Chemical and Biomolecular Engineering, Department of Chemistry and Biomolecular Science, and Center for Advanced Materials Processing (CAMP), 8 Clarkson Avenue, Clarkson University, Potsdam, New York 13699-5705

A new type of nanopore sensor design is reported for a reagent-less electrochemical biosensor with no analyte "tagging" by fluorescent molecules, nanoparticles, or other species. This sensor design involves immobilization within Au-coated nanopores of bacterial periplasmic binding proteins (bPBP), which undergo a wide-amplitude, hinge−twist motion upon ligand binding. Ligand binding thus triggers a reduction in the effective thickness of the immobilized protein film, which is detected as an increase in electrolyte conductivity (decrease in impedance) through the nanopores. This new sensor design is demonstrated for glucose detection using a cysteine-tagged mutant (GGR Q26C) of the galactose/glucose receptor (GGR) protein from the bPBP family. The GGR Q26C protein is immobilized onto Au nanoislands that are deposited within the pores of commercially available nanoporous polycarbonate membranes.

The use of nanomaterials, including nanowires, nanoparticles, and nanotubes, for the development of electrochemical biosensors has been recently reviewed.[1−3] The use of nanomaterials can be useful for enabling miniaturization, allowing the size of individual sensors in a sensor array to be minimized. In addition, the optical, electronic, or chemical properties of nanomaterials can often be tailored through control of their size. When proteins are incorporated as the biorecognition element in an electrochemical biosensor, the close correspondence between the protein size and the nanomaterial size can also be exploited.

We report here a new design paradigm for a reagent-less electrochemical biosensor using Au-coated nanopores from commercial nanoporous polycarbonate membranes within which a bacterial periplasmic binding protein (bPBP) is immobilized. The glucose/galactose receptor (GGR) protein, which is a member of the bPBP superfamily, has found widespread use as the biorecognition element in glucose biosensors based on fluorescence, quartz crystal microbalance, electrochemical impedance, and surface plasmon resonance detection.[4−14]

This protein is an ideal candidate for the active element in a glucose biosensor because it has a high solubility and is stable up to 60 °C. Most important, proteins from this superfamily undergo a wide-amplitude, hinge−twist motion upon ligand binding. This large physicochemical change upon ligand binding can then be detected using a variety of analytical techniques. The wild-type GGR protein contains no cysteine residues, but genetic engineering of GGR to introduce cysteine residues allows protein immobilization onto an Au surface through Au−S bond formation.[9,11−13] For our purposes, we have utilized GGR Q26C, a genetically engineered mutant with a single cysteine residue replacing the glutamine residue at position 26.[9,11] The GGR Q26C protein is illustrated in Figure 1.

The structural properties of the unliganded and liganded GGR have been investigated by thermal unfolding of the protein monitored by UV CD, fluorescence, and differential scanning calorimetry.[7,15,16] Sokolov et al. have shown by atomic force

* To whom correspondence should be addressed. Telephone: (315) 268-4471. E-mail: isuni@clarkson.edu.

[†] Department of Chemical and Biomolecular Engineering.

[‡] Department of Chemistry and Biomolecular Science.

[§] Current address: 319 Hudson Hall, SUNY at Plattsburgh, Plattsburgh, NY 12901.

(1) Wang, J. *Electroanalysis* **2005**, *17*, 7−14.
(2) Wang, J. *Analyst* **2005**, *130*, 421−426.
(3) Zhao, Q.; Gan, Z.; Zhuang, Q. *Electroanalysis* **2002**, *14*, 1609−1613.
(4) Marvin, J. S.; Hellinga, H. W. *J. Am. Chem. Soc.* **1998**, *120*, 7−11.
(5) Tolosa, L.; Gryczynski, I.; Eichhorn, L. R.; Dattelbaum, J. D.; Castellano, F. N.; Rao, G.; Lakowicz, J. R. *Anal. Biochem.* **1999**, *267*, 114−120.
(6) Benson, D. E.; Conrad, D. W.; de Lorimier, R. M. S.; Trammell, A.; Hellinga, H. W. *Science* **2001**, *293*, 1641−1644.
(7) Salins, L. L .E.; Ware, R. A.; Ensor, C. M.; Daunert, S. *Anal. Biochem.* **2001**, *294*, 19−26.
(8) De Lorimier, R. M.; Smith, J. J.; Dwyer, M. A.; Looger, L. L.; Sali, K. M.; Paavola, C. D.; Rizk, S. S.; Sadigov, S. D.; Conrad, W.; Loew, L.; Hellinga, H. W. *Protein Sci.* **2002**, *11*, 2655−2675.
(9) Luck, L. A.; Moravan, M. J.; Garland, J. E.; Salopek-Sondi, B.; Roy, D. *Biosens. Bioelectron.* **2003**, *19*, 249−259.
(10) Ye, K.; Schultz, J. S. *Anal. Chem.* **2003**, *75*, 3451−3459.
(11) Carmon, K. S.; Baltus, R. E. Luck, A. *Biochemistry* **2004**, *43*, 14249−14256.
(12) Hsieh, H. V.; Pfeiffer, Z. A.; Amiss, T. J.; Sherman, D. B.; Pitner, J. B. *Biosens. Bioelectron.* **2004**, *19*, 653−660.
(13) Wang, J.; Carmon, K. S.; Luck, L. A.; Suni, I. I. *Electrochem. Solid-State Lett.* **2005**, *8*, 61−68.
(14) De Lorimier, R. M.; Tian, Y.; Hellinga, H. W. Binding and signaling of surface-immobilized reagentless fluorescent biosensors derived from periplasmic binding proteins. *Protein Sci.* In press.
(15) Piszczek, G.; D'Auria, S.; Staiano, M.; Rossi, M.; Ginsburg, A. *Biochem. J.* **2004**, *381*, 97−103.
(16) Butler, S. L.; Falke, J. J. *Biochemistry* **1996**, *35*, 10595−10600.

10.1021/ac061319q CCC: $37.00
Published on Web 12/23/2006

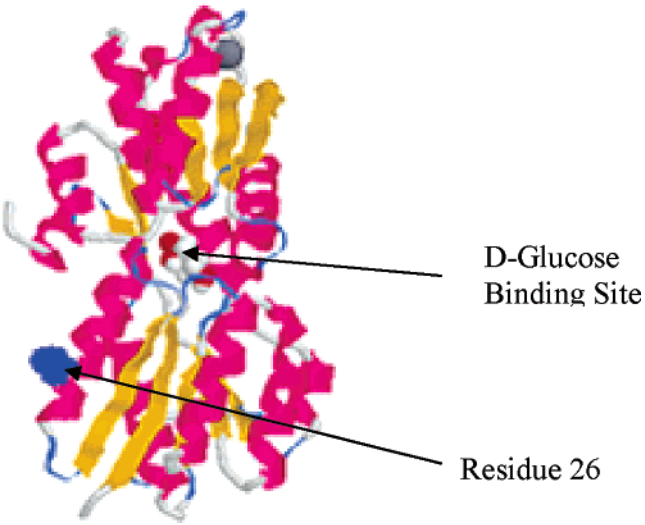

Figure 1. Illustration of the GGR Q26C protein, including the D-glucose binding site and mutation site.

Table 1. Polycarbonate Track-Etched Membranes Studied Here

pore diameter (nm)	pore density (cm^{-2})	thickness (μm)
10	6×10^8	6
30	6×10^8	6
100	4×10^8	6

microscopy (AFM) that the large conformational change upon glucose binding dramatically impacts the size and mechanical properties of the GGR protein.[17] The reduction in protein size upon ligand binding is exploited here to demonstrate a biosensor by immobilizing the GGR Q26C protein within an array of electrolyte-filled nanopores and detecting the conductivity change upon glucose binding. The GGR Q26C protein is immobilized onto the inner surface of polycarbonate nanopores by depositing Au nanoislands and then forming Au−S bonds to cysteine-modified proteins.

EXPERIMENTAL SECTION

Materials. Polycarbonate track-etched membranes with several different pore sizes were purchased from SPI Supplies, as summarized in Table 1.

Formaldehyde, ammonium hydroxide, sulfuric acid, nitric acid, and methanol were obtained from J. T. Baker and used as received. Tin chloride(II), sodium sulfite, silver nitrate, potassium chloride, Tris buffer, and calcium chloride were obtained from Sigma Aldrich and used as received. Trifluoroacetic acid was obtained from Superclo. Doubly distilled, deionized water was freshly prepared and used for all experiments. Commercial electroless Au plating solution (Oromerse Part B, Technic Inc.) was used as an Au plating bath after a 40 times dilution.

Expression and Purification of GGRQ26C. The GGR Q26C plasmid were expressed in BL21(DE3) cells and purified as described previously.[11] The final buffer for the experiments contains 100 mM KCl, 10 mM Tris pH 7.1, and 0.5 mM $CaCl_2$. The protein concentration for these experiments was 27 μM.

(17) Sokolov, I.; Venkatesh, S.; Luck, L. A. *Biophys. J.* **2006**, *90*, 1055−1063.

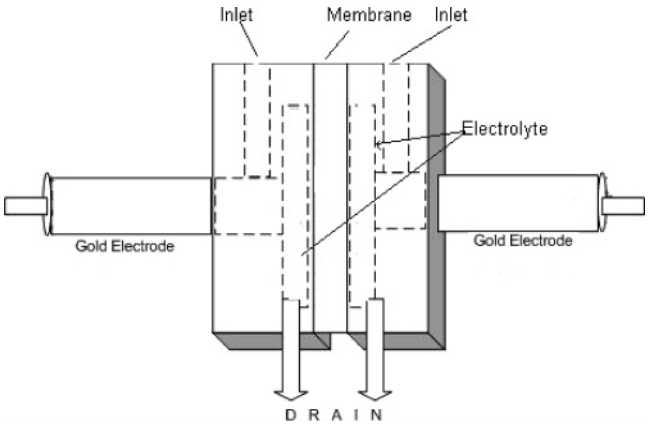

Figure 2. Schematic of the electrochemical cell used for impedance measurements.

Gold Nanoisland Preparation. Template synthesis of nanostructures, as developed in the laboratory of Martin, was used to create a discontinuous layer of Au nanoislands on the inner walls of a nanoporous polycarbonate membrane.[18,19] The pH was reduced to 10 and the temperature of the plating bath was reduced to 0−4 °C to reduce the Au deposition rate and prevent formation of continuous Au nanotubes. The polycarbonate membranes were immersed in the electroless Au plating bath for 2 h and 30 min. The same electroless plating bath and conditions were used for polycarbonate membranes with different pore sizes (10, 30, and 100 nm). As discussed below, this procedure forms discontinuous Au nanoislands.

Cell Design. A schematic representation of the electrochemical cell is shown in Figure 2.

The cell design consists of two identical virgin Teflon blocks with a cylindrical bore along the center. Two Au electrodes of area 0.0177 cm^2 from SPI Supplies were mounted at each end of the cell. The Au-coated membrane was mounted between the two Teflon blocks using a Chemraz O-ring. The total cell volume was ~1800 μL, divided equally on both sides of the membrane. Fluid inlet and drain were incorporated on both sides of the membrane to rapidly replace the electrolyte. The impedance measured between the two Au electrodes can be considered as three resistances in series, R_A, R_M, and R_B. R_A and R_B correspond to the electrolyte resistance between the two Au electrodes and the membrane, while R_M corresponds to the electrolyte resistance within the Au/polycarbonate nanopores.

Instrumentation. Impedance measurements were obtained at a fixed frequency of 1 kHz with one Au electrode serving as the working electrode and the other Au electrode serving as both counter and reference electrodes. The impedance that is obtained is almost purely real and is directly (inversely) proportional to the resistance (conductivity) between the two Au electrodes. The dc potential and 10-mV ac probe voltage were applied by a Princeton Applied Research (PAR) model 263A potentiostat, and phase-sensitive detection was accomplished with a Stanford Research Systems SR830 lock-in amplifier. The impedance values were recorded once every 5 min for the duration of the experiment. To avoid doing unwanted electrochemistry, the potentiostat is turned off between measurements.

(18) Martin, C. R.; Nishizawa, M.; Jirage, K.; Kang, M. *J. Phys. Chem. B* **2001**, *105*, 1925−1934.
(19) Menon, V. P.; Martin, C. R. *Anal. Chem.* **1995**, *67*, 1920−1928.

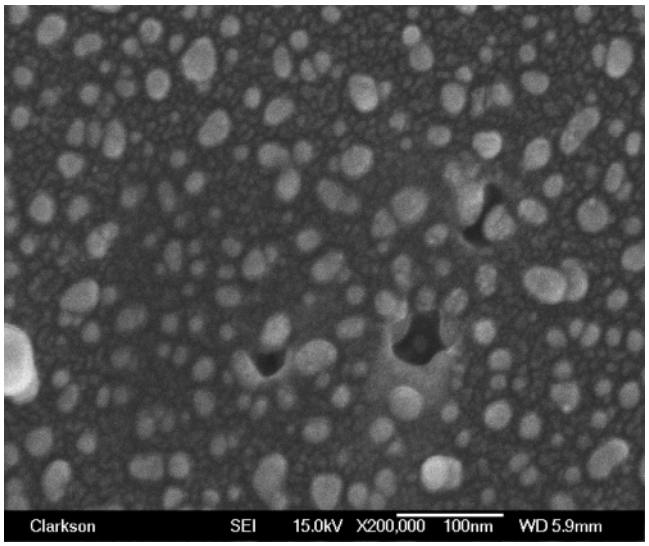

Figure 3. SEM image of the top surface of a polycarbonate membrane with 30-nm-diameter pores after electroless Au deposition for 2 h and 30 min.

Protein Immobilization and Electrolyte Addition. To aid wetting, the polycarbonate Au template is first immersed into a 10 mM Tris solution for 2 h. Onto one face of the membrane, 180 μL of GGR Q26C solution is added dropwise with a micropipet. The protein is allowed to diffuse into and immobilize onto the membrane pores for 60 min. To remove nonchemisorbed protein, the membrane is rinsed carefully by pouring 100 mM KCl, 10 mM Tris pH 7.1, 0.5 mM $CaCl_2$ buffer slowly across the membrane surface. After assembly of the electrochemical cell, the cylindrical channel through the center is filled with 100 mM KCl, 10 mM Tris pH 7.1, 0.5 mM $CaCl_2$ buffer, and impedance measurements are taken for 60−80 min to ensure that the system is at steady state. To alter the D-glucose concentration, the old electrolyte is drained dropwise from the bottom while the new electrolyte is simultaneously added dropwise to the top. The new electrolyte differs from the old electrolyte only in the addition of D-glucose to the desired concentration. This entire cell volume is replaced three times to ensure the desired D-glucose concentration is reached.

RESULTS AND DISCUSSION

Figure 3 shows a SEM image of the top surface of a polycarbonate membrane with 30-nm-diameter pores after 2 h and 30 min of electroless Au deposition, illustrating the formation of Au nanoislands 8−35 nm in diameter. Approximately 45% of the polycarbonate surface is covered with Au nanoislands, and a similar surface coverage is expected within the nanopores. The electroless Au deposition process was deliberately interrupted before a continuous Au film formed and Au nanotubes were created. The formation of continuous Au nanotubes might provide an alternative conductive pathway that would complicate the impedance measurements.

The protein is then immobilized on this discontinuous gold film. Test experiments with fructose, a sugar that is not recognized by the GGR protein, were conducted to ensure that the electrolyte replacement procedure does not alter the measured impedance. Figure 4 shows the impedance change upon introduction of 2 mM

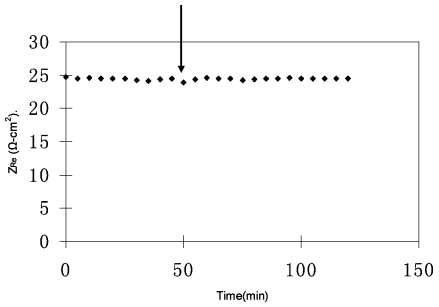

Figure 4. Real component of the impedance (Z_r) at 1 kHz after addition of 2 mM fructose to the GGR Q26C-immobilized, Au-plated polycarbonate membrane with a 30-nm pore size. The arrow indicates the time when fructose was introduced.

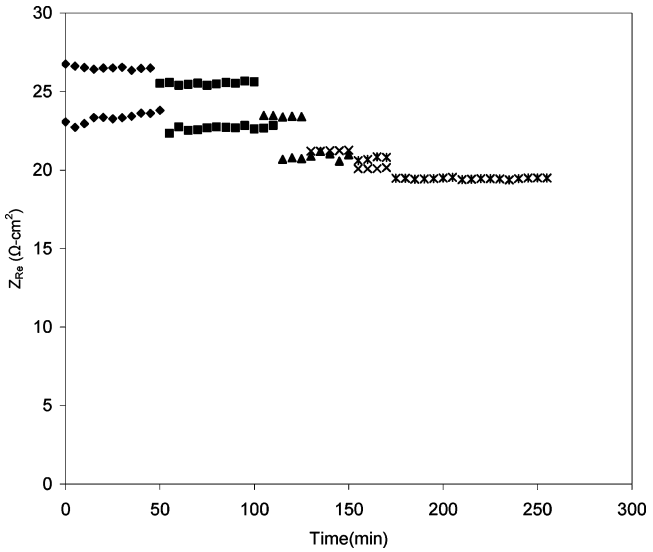

Figure 5. Real component of the impedance change (Z_{Re}) at 1 kHz for increasing concentrations of D-glucose. Data are shown for no glucose (◆) and 40 (■), 70 (▲), 100 (×), and 200 μM glucose (∗). The top data set corresponds to a pore of 10 nm diameter, and the bottom set to a pore diameter of 30 nm.

fructose into the electrochemical cell, showing that the impedance is the same before and after fructose introduction. This verifies that the electrolyte replacement procedure does not introduce spurious changes in the measured impedance and also verifies that fructose does not bind to the immobilized GGR Q26C protein.

Figure 5 illustrates the real component of the impedance change at 1 kHz for several stepwise increases in D-glucose concentration for both 10- and 30-nm-diameter pores. In both cases, the impedance decreases continuously as the D-glucose concentration is increased. This corresponds to a decrease in the impedance (resistance) of the electrolyte within the membrane nanopores as the protein "folds up" around the glucose ligand, increasing the effective diameter of the nanopores and thereby decreasing their resistance.

During both experiments shown in Figure 5, the Au electrode positions are unchanged, so R_A and R_B are constant. Only R_M is affected by the introduction of D-glucose, with R_M decreasing as the effective diameter of the nanopores increases. Recent AFM studies of the GGR Q26C protein by Sokolov et al. further illuminate the results of Figure 5.[17] The results from the AFM studies show that the protein film thickness was effectively decreased by ~2 nm when saturated with glucose. This is clearly

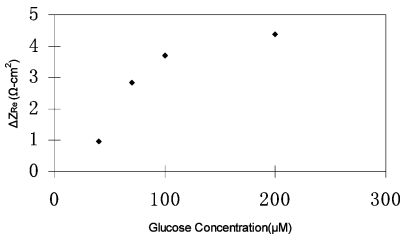

Figure 6. Change in the real component of the impedance (ΔZ_{Re}) as a function of D-glucose concentration for GGRQ26C-immobilized, Au-plated polycarbonate membrane with a 30-nm pore size.

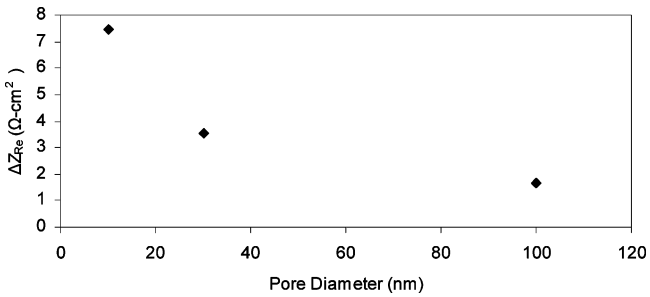

Figure 7. Drop in the real component of the impedance upon introduction of 2 mM D-glucose for three different membrane pore diameters (10, 30, and 100 nm).

consistent with the decrease in R_M obtained in Figure 5 upon glucose binding. Other analytical techniques have also shown protein dimensional changes of 1−2 nm for proteins from the bacterial periplasmic binding protein (PBP) family.[9,20]

The results from Figure 5 for 30-nm-diameter pores are presented in Figure 6 as the impedance change as a function of D-glucose concentration. Figure 6 shows the expected saturation behavior of the impedance change at D-glucose concentrations higher than the glucose equilibrium dissociation constant (K_d), which is ~0.2 μM for the protein in soluble form.[21] One might be tempted to calculate a value of K_d for the Au-immobilized GGR Q26C protein from the results shown in Figure 6. However, this may not be very accurate, given the indirect relationship of this measurement. Figure 6 is presented merely to illustrate that the results obtained with the current sensor arrangement are physically reasonable. It should be noted that the glucose dissociation constant for the GGR protein can be increased into the physiologically significant range (1−30 mM) for glucose detection through residue substitution near the ligand binding pocket.[12]

The results of Figure 5 can be compared in terms of trends in the impedance response with the effective nanopore diameter. However, this trend is complicated by the design of the electrochemical cell shown in Figure 2, which does not control the exact position of the two Au electrodes. As a result, the two resistances R_A and R_B vary between different experiments, complicating comparisons between different nanopore diameters. Upon glucose introduction, only the resistance R_M is affected, and this depends on nanopore diameter (d), diameter of membrane exposed to the electrolyte (D), nanopore density (ρ), and membrane thickness (t) according to

$$R_M = \frac{t}{\kappa\rho\left(\frac{\pi}{4}d^2\right)\left(\frac{\pi}{4}D^2\right)} \quad (1)$$

where κ is the electrolyte conductivity. The change in R_M upon glucose introduction should be

$$\Delta R_M = \frac{16t}{\pi^2\kappa\rho D^2}\left[\frac{1}{d^2} - \frac{1}{(d+\Delta d)^2}\right] \quad (2)$$

Here d must be viewed as the effective inside pore diameter prior to glucose binding, and Δd is the change in effective pore diameter upon glucose binding.

The value for d is equal to the nanopore diameter minus the effective thickness of the Au nanoislands and the effective thickness of the immobilized protein. Uncertainties in these values and in the fractional surface coverage of both Au and GGR protein preclude direct numerical calculation of Δd from the results of Figure 5. Equation 2 is given only for the purpose of illustrating the expected mechanism of this sensor. Δd_i in eq 2 would be ~2 × 2 nm upon glucose binding for complete surface coverage of both Au and GGR protein.

Thus, direct application of eq 2 to the results of Figure 5 is complicated by the following factors: uncontrolled variations in R_A and R_B; the differences shown in Table 1 between t, ρ, and d for the different membranes; and uncertainty in the effective thickness and surface coverage of both the Au nanoislands and the GGR protein. Despite the complications of quantitative application of eq 2, some overall trends can be tested. For example, the change in effective diameter should increase as the nanopore diameter decreases. Figure 7 shows the results of measurements for the total impedance change upon introduction of 2 mM D-glucose. The expected trend is observed, that the greatest sensitivity is attained with the smallest diameter nanopores.

The results shown in Figure 7 provide some insight into the site of protein adsorption. The GGR protein shown in Figure 1 has a major axis of ~6.5 nm and a minor axis of ~3.5 nm, as found from crystallography.[22] Thus, GGR protein may be immobilized within the 10-nm-diameter pores within the polycarbonate membrane, although the biosensor response for the 10-nm pores may also arise in part from protein immobilized at or near the pore mouth. On the other hand, the 100-nm pore size is considerably larger than the protein size, so diffusion and subsequent protein immobilization within these pores should be facile.

These results demonstrate the potential for creating a reagentless biosensor with no "tagging" by fluorescent species, nanoparticles, metallization, or insoluble product formation.

CONCLUSIONS

A cysteine-tagged mutant (GGR Q26C) of the GGR protein is employed to demonstrate a reagent-less biosensor for glucose. The GGR Q26C protein is immobilized within the pores of commercially available polycarbonate membranes onto which Au

(20) Mowbray, S. L., Sandgren, M. O. J. *J. Struct. Biol.* **1998**, *124*, 257−275.
(21) Vyas, M. N.; Vyas, N. K.; Quiocho, F. A. *Biochemistry* **1994**, *33*, 4762−4768.
(22) Vyas, N. K.; Vyas, M. N.; Quiocho, F. A. *Science* **1988**, *242*, 1290−1295.

nanoislands have been deposited. This allows protein film growth through formation of covalent Au−S bonds. Glucose can be detected as a decrease in the impedance through the electrolyte within the nanopores as the effective protein film thickness is reduced. This thickness reduction arises from the well-characterized hinge−twist motion of the GGR protein upon glucose binding.

For pore sizes of 10 and 30 nm, the impedance response is shown to scale with glucose concentration according to the glucose dissociation constant of the GGR protein. For pore sizes of 10, 30, and 100 nm, the sensitivity is shown to decrease with increasing pore size. These results demonstrate a new type of nanobiosensor design in which bPBPs, which undergo wide-amplitude motion upon ligand binding, are immobilized within Au-coated nanopores, and ligand binding is detected as an increase in the electrolyte conductivity within the nanopores caused by the reduction in the effective protein film thickness.

ACKNOWLEDGMENT

This research was supported by National Science Foundation grants CTS-0329698 and CCF-0304143.

Received for review July 20, 2006. Accepted October 26, 2006.

AC061319Q